Mechanism of Partial Agonism at the GluR2 AMPA Receptor: Measurements of Lobe Orientation in Solution[†]

Alexander S. Maltsev,[‡] Ahmed H. Ahmed,[‡] Michael K. Fenwick,[‡] David E. Jane,[§] and Robert E. Oswald*[,‡]

Department of Molecular Medicine, Cornell University, Ithaca, New York 14853, and Department of Physiology and Pharmacology, MRC Centre for Synaptic Plasticity, School of Medical Sciences, University of Bristol, Bristol BS8 1TD, U.K.

Received May 8, 2008; Revised Manuscript Received August 11, 2008

ABSTRACT: The mechanism by which the binding of a neurotransmitter to a receptor leads to channel opening is a central issue in molecular neurobiology. The structure of the agonist binding domain of ionotropic glutamate receptors has led to an improved understanding of the changes in structure that accompany agonist binding and have provided important clues about the link between these structural changes and channel activation and desensitization. However, because the binding domain has exhibited different structures under different crystallization conditions, understanding the structure in the absence of crystal packing is of considerable importance. The orientation of the two lobes of the binding domain in the presence of a full agonist, an antagonist, and several partial agonists was measured using NMR spectroscopy by employing residual dipolar couplings. For some partial agonists, the solution conformation differs from that observed in the crystal. A model of channel activation based on the results is discussed.

The majority of excitatory synaptic transmission in the vertebrate central nervous system is mediated by ionotropic glutamate receptors (iGluRs)[1] (*3*). These receptors also play important roles in neuronal development and the formation of synaptic plasticity underlying higher-order processes such as learning and memory (*4*). In addition, iGluRs are also associated with neurologic disorders, including epilepsy and ischemic brain damage, and neurodegenerative disorders such as Huntington's chorea, Parkinson's disease, and Alzheimer's disease. iGluRs are membrane-bound receptor ion channels composed of four subunits surrounding a central ion channel in which each subunit contributes to pore formation. Subunits are categorized by pharmacological properties, sequence, functionality, and biological role into those that are sensitive (1) to the synthetic agonist α-amino-3-hydroxy-5-methyl-4-isoxazolepropionic acid (AMPA; GluR1-4), (2) to the naturally occurring neurotoxin kainate (GluR5-7, KA1,2), and (3) to the synthetic agonist *N*-methyl-D-aspartic acid (NMDA; NR1, NR2A-D, NR3A-B).

The three-dimensional structures of the binding domain (S1S2) of a number of glutamate receptors are known from X-ray crystallography. In particular, the structures of GluR2 bound to a wide variety of agonists, partial agonists, and antagonists have provided compelling clues about the structural basis of channel activation (*5*) and desensitization (*6*). The binding domain consists of two weakly interacting lobes with the agonist-binding site between the lobes (*7*). The binding of agonists and partial agonists results in a closure of the lobes. At least in some cases, the degree of lobe closure is smaller with partial agonists than with full agonists, and the suggestion has been made that the degree of lobe closure is correlated with the efficacy of the partial agonist (*5*). This apparent correlation does not directly yield structural insight for several reasons. First, the intact receptor is composed of four subunits, all with agonist binding sites, and the occupation of these four sites has to be considered in any model of activation. Second, single-channel studies have found that at least three conductance levels can be observed and that partial agonists activate the same conductance levels as full agonists (the lower conductance levels are preferentially populated by partial agonists). Finally, the degree of lobe closure as observed in X-ray structures is affected by the crystallization conditions such that crystals formed in high concentrations of zinc are often found to exhibit a higher degree of lobe closure than those formed in the absence of zinc. One can equally argue that zinc distorts the structure, that zinc stabilizes the native structure, or that the presence or absence of zinc reveals at least a portion of the range of relative motion of the two lobes.

In order to restrain potential models for the structural basis of activation of AMPA receptors, understanding the structural and dynamic differences of the binding domain bound to partial agonists is crucial. In addition to the crystal structures, the internal dynamics of each lobe have

[†] This work was supported by grants from the National Institutes of Health (R01-GM068935) and the National Science Foundation (IBN-0323874). Travel funds were provided by the Abraham and Henrietta Brettschneider Oxford and Cornell Exchange Fund. The chemical synthesis of willardiine derivatives was supported by a grant from the Medical Research Council, U.K.

* To whom correspondence should be addressed. Telephone: (607) 253-3877. Fax: (607) 253-3659. E-mail: reo1@cornell.edu.

[‡] Cornell University.

[§] University of Bristol.

[1] Abbreviations: AMPA, α-amino-3-hydroxy-5-methyl-4-isoxazolepropionic acid; BrW, (*S*)-5-bromowillardiine; ClW, (*S*)-5-chlorowillardiine; FW, (*S*)-5-fluorowillardiine; HW, (*S*)-willardiine {(*S*)-2-amino-3-[3,4-dihydro-2,4-dioxopyrimidin-1(2*H*)-yl]propanoic acid}; iGluR, ionotropic glutamate receptor; IW, (*S*)-5-iodowillardiine; IPTG, isopropyl β-D-thiogalactoside; NW, (*S*)-5-nitrowillardiine; NMDA, *N*-methyl-D-aspartic acid; S1S2, extracellular ligand-binding domain of GluR2; RDC, residual dipolar coupling; UBP277, (*S*)-3-(2-carboxyethyl) willardiine.

10.1021/bi800843c CCC: $40.75
Published on Web 09/17/2008

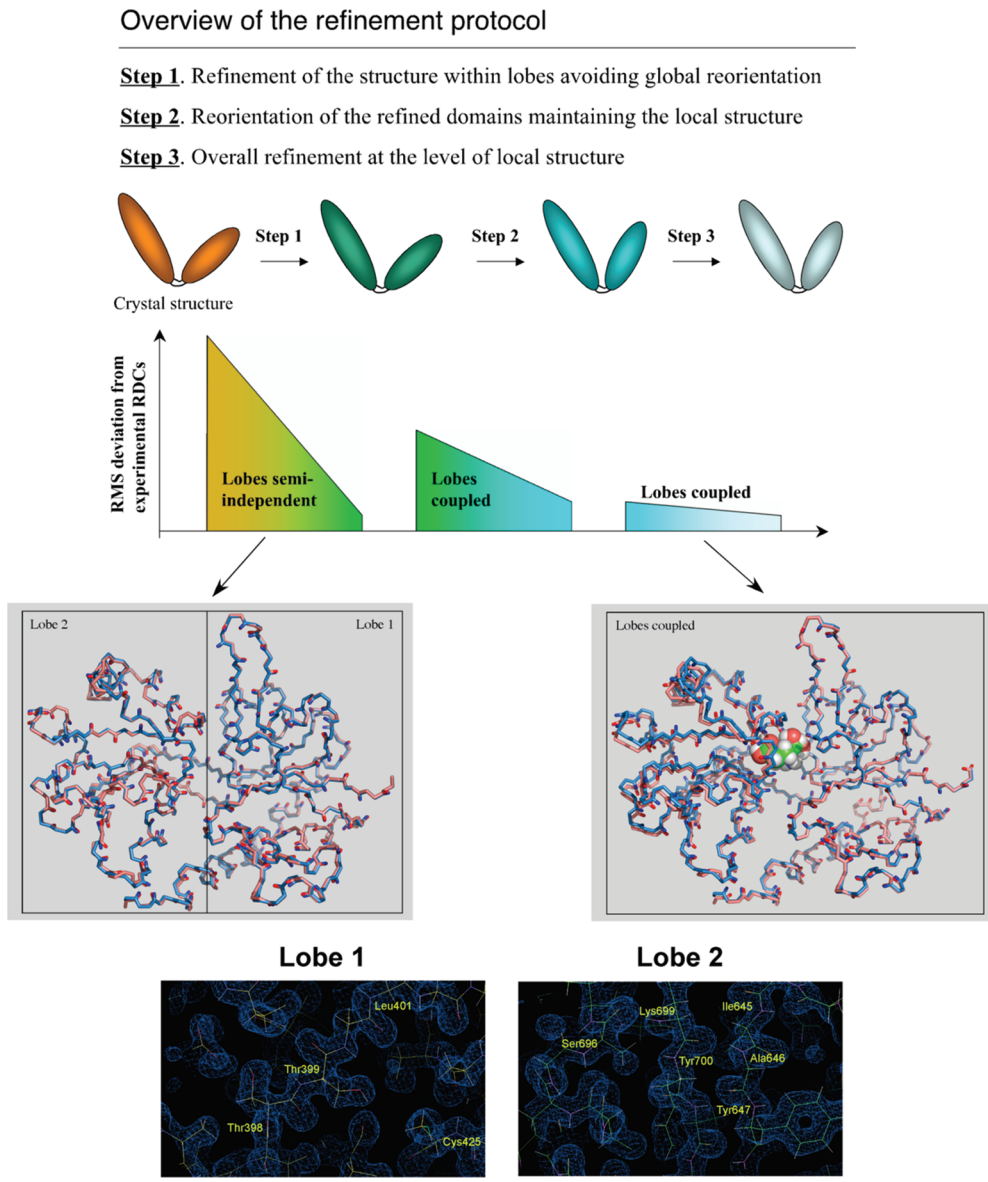

FIGURE 1: Overview of the refinement protocol. In the first step, the RDCs are used to refine the orientation of the NH bond vectors within each lobe independently to remove structural noise. This employs data from five alignment media (for each medium, two alignment frames, one for each lobe, are used). Although the fit of the measured RDCs to the calculated RDCs is improved dramatically, this results in only a subtle reorientation of the NH bond vectors as shown illustrated by the structures at the bottom left. The pink structure corresponds to the glutamate-bound crystal structure (PDB entry 1ftj), with the amide protons colored red. The light blue structure is the structure refined by RDCs in the first step, with the amide protons colored blue. No global movements of the lobes are made in this step. Following local refinement, one alignment frame for each medium is used to reorient the lobes for consistency with the RDC measurements. The last step also uses one alignment frame per medium and allows both the global and local structure to be refined simultaneously. The result is shown in the structure at the bottom right (coloring is the same as in the structures at the left). Glutamate is shown in the binding site as a space-filling model. Lobe 1 of the crystal structure and lobe 1 of the RDC-refined structure are aligned. In the bottom panels, the RDC-refined glutamate-bound structure fits within the electron density map of the crystal structure of the glutamate-bound form of GluR2 S1S2 (PDB entry 3dp6), both when lobe 1 is superimposed on the crystal structure (left) and when lobe 2 is superimposed (right).

been studied with NMR spectroscopy (*8*−*11*) and the relative strengths of hydrogen bonds have been accessed with FTIR (*12*−*14*) and NMR (*9*) studies. The overall picture is that lobe 1 (Figure 1) is relatively rigid on the micro- to millisecond time scale, with lobe 2 exhibiting characteristic internal motions that vary between those of full and partial agonists (*8*−*11*). Both NMR spectroscopy (*8*) and computational methods (*15*−*17*) suggest that the relative orientation of the lobes is variable in the apo and some antagonist-bound states and that upon binding of full agonist, a more stable orientation is achieved.

Using solution NMR spectroscopy, additional structural information can be obtained from residual dipolar couplings (RDCs) that are measured in weakly aligning media (*18, 19*). RDCs can be used to constrain the orientation of bond vectors (in this case, NH bond vectors) and provide unique structural information. In the case of GluR2 S1S2, we show here that the average relative orientation of the two lobes can be determined in the solution state and, in some cases, differs significantly from the orientation measured from the crystal structures. Also, the conformational equilibrium of a characteristic conformational shift in lobe 2 (peptide flip region)

can be determined with RDCs. These findings have important implications for models of channel activation.

EXPERIMENTAL PROCEDURES

Materials. Kainate, IW, and FW were obtained from Tocris (St. Louis, MO). Other willardiine compounds were synthesized as described previously (*20, 21*). The GluR2 S1S2J construct was obtained from E. Gouaux (Vollum Institute) (*1*).

Protein Preparation and Purification. The GluR2 (flop) S1S2 domain consists of residues N392−K506 and P632−S775 of the full-length rat subunit (*22*), a "GT" linker connecting K506 and P632 (*1*), and a "GA" segment at the N-terminus. The polyhistidine-tagged protein was expressed (37 °C) in inclusion bodies [BL-21(DE3) *Escherichia coli*], refolded, treated with trypsin for removal of the histidine tag, and purified (*10, 23*). Isotopically enriched, fully deuterated, minimal media (1.25 L) (*24*) yielded three or four samples of 0.25−0.35 mM purified protein. Deuteration was achieved by dissolving lyophilized medium components in pure D_2O and culturing with deuterated glucose. Exchange of deuterons for protons at labile sites occurred following lysis in aqueous refolding and purification buffers. The resulting protein had protons on the nitrogen atoms and deuterons on the carbons. The NMR buffer was an aqueous solution of 25 mM sodium acetate, 25 mM sodium chloride, 1 mM sodium azide, and 12% D_2O (pH 5.0). Final concentrations of FW, NW, ClW, BrW, IW, and UBP277 were 3 mM. Final concentrations of HW and kainate were 11 mM. Ligands were exchanged using successive dilution and concentration using an Amicon Ultra-4 (10K) filter.

NMR Spectroscopy. All measurements were taken on a Varian Inova 500 spectrometer equipped with a triple-resonance, z-gradient cryogenic probe. The standard $^{1}H-^{15}N$ TROSY experiment in BioPack (Varian, Palo Alto, CA) was used, successively selecting, by modification of the phase cycle, the bottom right and top right peaks to provide the nitrogen coupling. The difference in hertz between the chemical shifts of the peaks for any given amide in these two spectra provides the nitrogen coupling. The difference in the nitrogen coupling between the unaligned and aligned spectra for each set of peaks provides the RDC value in hertz (representative spectra are shown in Figure S1 of the Supporting Information). Spectra were recorded at 25 °C and processed using NMRPipe version 1.6 (*25*). The data were apodized with a mixed exponential-Gauss window function and zero-filled to double the original number of data points before Fourier transformation. Spectra were displayed and the peaks chosen and measured using Sparky (*26*).

Measurements of NH RDCs were taken in five different alignment media for S1S2 bound to the full agonist glutamate [alkyl-PEG(C12E5)/hexanol (*27*), DLPC/CHAPSO (*28*), neutral acrylamide gel (*29*), cetylpyridinium chloride/hexanol/NaCl (*30*), and positively charged acrylamide gel (*31*)]. The first three media are neutral and were expected to display a steric mechanism of alignment. Indeed, the RDCs measured in these media were strongly correlated. On the other hand, the cetylpyridinium chloride/hexanol/NaCl medium and the charged gel are both positively charged and were expected to display a coulombic mechanism of alignment. RDCs were strongly correlated in these two media, but much more weakly correlated with the three neutral media.

Structure Refinement Using NH RDCs. All calculations were performed in the molecular structure determination package Xplor-NIH incorporating features related to RDCs (*32*). NH RDCs from the glutamate−S1S2 structure were used to produce a structure with low structural noise and a lobe orientation consistent with the measured RDCs (Figure 1). A single measured RDC corresponds to a continuum of possible internuclear vector orientations, so that the structure of a protein cannot be optimized precisely. For this reason, multiple alignment media are required. Previous work has shown theoretically that RDCs from three independent media are enough to refine a structure (*33*). As described above, we have used five different alignment media to obtain five measures of NH RDC for each residue. Because three of the media align the protein by a steric mechanism [alkyl-PEG(C12E5)/hexanol (*27*), DLPC/CHAPSO (*28*), and neutral acrylamide gel (*29*)] and two by an electrostatic mechanism [cetylpyridinium chloride/hexanol/NaCl (*30*) and positively charged acrylamide gel (*31*)], the data sets obtained are not necessarily independent. Using singular-value decomposition (*33*), the data from the five media were found to correspond to three independent data sets (two very precise and one somewhat less precise).

Thus, the data provided both independent measures of the RDC and redundant measures in independently prepared samples. Only RDCs obtained from the reliably resolved peaks were used. Lobe 1 was defined as residues 392−496 and lobe 2 residues 501−506 and 633−727. Peaks corresponding to residues that were recognized as significantly dynamic were not used in refinement (*9, 11*). Residues 730−775, which would normally be considered a part of lobe 1, were not used in refinement because of the potential of that segment for global reorientations with respect to the rest of lobe 1. In total, 121 NH bonds were refined: 61 in lobe 1 and 60 in lobe 2. The first step of refinement started with a crystal structure and used two alignment tensors for each medium, one for each lobe (Figure 1). The magnitude and rhombicity of the two tensors were constrained to be equal. The overall structure was maintained by placing restraints (±0.1 Å) on the distance between every pair of C^{α} atoms separated by <15 Å. This procedure has little effect on the overall structure of the protein, with an only 0.2 Å deviation between the original and optimized C^{α} coordinates. However, the rmsd of the experimental versus calculated RDC values decreased on average from 4.08 to 0.79 Hz, and the *R* value improved from 21.5 to 3.6%. The optimized lobes were then reoriented on the basis of the RDC data while the internal structure of each lobe was kept constant. The last step consisted of optimizing the structure as in the first step, but in this case, using only one alignment tensor per medium. The three-step optimization procedure was performed starting from seven substantially different structures [PDB entries 1ftj (chains A, B, and C), 1fw0, and 1ftm (chains A, B, and C)]. To determine the lobe orientation of the partial agonists and antagonist, only the second step in the refinement protocol was used. This step reorients the lobes as rigid bodies, using only the NH bonds that were previously refined in the glutamate−S1S2 data set. As shown in Table 2, this rigid body reorientation of the glutamate−S1S2 structure optimized with RDCs fits the RDC data for each

Table 1: Statistics Describing the Fit of the RDC Data to a Refined and Nonrefined Glutamate Structure (1ftj, A chain)[a]

	fit for reoriented nonrefined structure				fit for reoriented refined structure			
medium	Da (Hz)	Rh	rms (Hz)	*R* factor	Da (Hz)	Rh	rms (Hz)	*R* factor
C12E5/hexanol	−12.02	0.454	3.40	20.8	−13.74	0.479	0.45	2.39
neutral gel	17.31	0.487	4.30	18.1	20.05	0.475	0.81	2.97
DLPC/CHAPSO	−9.60	0.556	2.69	20.0	−11.76	0.479	0.48	2.97
CPBr/hexanol	21.65	0.194	5.12	18.5	24.97	0.179	1.14	3.57
charged gel	11.68	0.190	3.79	25.3	14.21	0.205	1.11	6.09

[a] Da and Rh refer to the magnitude and rhombicity of the alignment tensor, and rms and *R* factor describe the variation between the predicted and observed RDC values.

willardiine better than the crystal structure obtained with the corresponding ligand.

RESULTS

Assignments. The backbone assignments for GluR2 S1S2 bound to willardiine (HW) and its halogenated derivatives have been reported previously (*34*). Since only well-structured regions of the protein were used for the analysis, the assignments for ClW- and NW-bound S1S2 could be made by comparison to the assignments of the protein bound to FW, BrW, and IW. Chemical shift changes relative to the parent HW compound are restricted to the peptide flip region and residues near the disulfide bond (*9, 34*). The antagonist, UBP277, exhibited considerable chemical shift changes, and the backbone assignments were made using a combination of HNCO, HNCOCA, and HNCA experiments with a fully deuterated, ^{15}N- and ^{13}C-labeled sample.

Lobe Orientation. (i) Optimization of the Glutamate Structure. Numerous crystal structures of the GluR2 S1S2 domain have been determined (e.g., refs *1, 5*−*7, 35*), and the overall structure of each lobe of the protein is well-documented. However, the relative orientation of the two lobes is variable in the presence of various agonists and antagonists, and potentially susceptible to crystal packing forces. The goal of this work is to attempt to determine the differences in lobe orientation between a full agonist glutamate and a group of other ligands with high precision to help constrain models of channel activation. The strategy is to rely on NH RDCs that are highly sensitive to rotations of domains within a protein.

Although RDC data can be obtained for a variety of bond vectors in a protein (*19, 28, 36*), NH RDCs were used because the NH RDC is large (relative to other backbone RDCs that can be measured using protein fully deuterated on carbon atoms; see Experimental Procedures) and can be measured with high precision via two-dimensional ^{1}H−^{15}N TROSY experiments. However, NH RDCs generally do not fit a typical X-ray structure within the estimated measurement errors due to the presence of "structural noise" (*37, 38*). Structural noise arises from the extreme sensitivity of RDCs to internuclear vector orientations, so that even very precise X-ray structures do not reflect the average solution conformation with sufficient precision for RDC work. This problem is further exacerbated for NH RDCs because hydrogen atoms are not directly observed in X-ray structures and have to be positioned computationally. The intrinsic dynamics of NH bonds can also be a source of structural noise, but in the case of GluR2 S1S2, this has been characterized extensively (*9*−*11*) and only NH bonds showing little or no internal dynamics on the micro- to millisecond time scale were used in this analysis. NH RDCs from a single medium are not sufficient for defining both the alignment frame and the orientation of specific vectors (see Experimental Procedures). For this reason, multiple alignment media were used to provide both independent and redundant measures of bond orientation.

S1S2 bound to the native neurotransmitter, glutamate, was used as a reference structure, which was calculated via a three-step optimization procedure starting from a crystal structure (Figure 1). In every step of the procedure, NH RDCs from five alignment media were used simultaneously. The first step reduced the structural noise by optimizing each lobe individually and preventing global reorientations (using separate semi-independent alignment tensors for each lobe and for each medium). That was followed by a rigid body rotation of the two lobes to place both lobes in the same alignment frame for each medium. Finally, a local optimization of the entire structure using only one alignment tensor per medium was performed. The first step removes much of the structural noise by reorienting the NH bond vectors to satisfy the RDC data. A comparison of the structures before and after step 1 (Figure 1) illustrates that the reorientation of the NH bond vectors within a lobe is small (Figure 1) and largely within the electron density map of an independently determined 1.55 Å crystal structure (*39*). Nevertheless, the improvement of fit to the data is dramatic (Table 1). The only experimental data used in the refinement procedure were NH RDCs. Since NH RDCs are sensitive to only the directions of the NH bond vectors, the refinement is an optimization of these vectors, while the actual positions of most of the atoms are not optimized in any way, but rather only kept similar to what was observed in the starting crystal structure. The possible orientations of NH vectors were further limited only by geometrical constraints on the configuration of peptide planes and by preventing steric clashes of N and H^N atoms with other atoms. These constraints are not very restrictive, and slight reorientation of an NH vector would be possible without breaking any constraints. Thus, the refinement procedure can be visualized as arriving at a set of NH vectors that best satisfy all the measured RDCs, while the actual protein structure is somewhat flexibly attached to the frame formed by NH vectors.

The procedure was performed with seven different starting crystal structures [glutamate-bound 1ftj (chains A, B, and C), kainate-bound 1fw0, and AMPA-bound 1ftm (chains A, B, and C)], and the final relative orientation of the two lobes differed by ±2° [calculated with DynDom (*2*)]. These differences were measured from comparison of the structures at the level of atom coordinates and are the consequence of

Table 2: Comparison of the Previously Obtained Crystal Structures (*1*, *5*, *49*; A. H. Ahmed et al., unpublished observations) with the Structures Refined with RDCs[a]

	crystal structures					structures refined with RDCs		
ligand	PDB	Zn	rms (Hz)	*R* factor (%)	relative degree of opening	rms (Hz)	*R* factor (%)	relative degree of opening
	1ftj	+	−	−	−	0.468 ± 0.068	2.48 ± 0.35	−
kainate		+	2.84 ± 0.30	15.9 ± 1.8	9.2 ± 0.01	1.11 ± 0.19	5.60 ± 0.99	11.35 ± 0.28
	1fw0	−	3.02	17.8	10.7			
HW	1mqj	+	3.25	12.8	3.85	1.51 ± 0.04	5.34 ± 0.19	3.85 ± 0.43
FW	1mqi	−	2.81	16.7	4.91	0.697 ± 0.042	3.66 ± 0.20	3.85 ± 0.77
ClW		+	3.33 ± 0.08	16.9 ± 0.3	3.38 ± 1.04	0.689 ± 0.081	3.10 ± 0.34	3.00 ± 0.53
NW		+	3.58 ± 0.39	17.9 ± 2.0	2.72 ± 1.1	1.06 ± 0.16	4.75 ± 0.69	3.38 ± 0.65
BrW	1my3	+	3.02 ± 0.04	18.7 ± 0.3	2.79 ± 1.63	1.11 ± 0.05	6.02 ± 0.28	4.86 ± 0.71
	1mqh	−	2.80	17.6	5.52			
IW	1my4	+	3.66 ± 0.89	22.2 ± 5.4	3.61 ± 1.37	0.959 ± 0.067	5.05 ± 0.34	5.30 ± 1.47
	1mqg	−	2.96 ± 0.10	17.8 ± 0.8	9.04 ± 0.48			
UBP277		+	2.86 ± 0.15	18.4 ± 1.1	19.8 ± 0.6	1.21 ± 0.11	6.81 ± 0.61	16.63 ± 0.57

[a] The rms and *R* factor refer to the comparison with the RDC data set for each S1S2−ligand complex. The relative degree of opening is determined relative to the glutamate-bound structure (PDB entry 1ftj; C protomer) for the crystal structures and relative to the corresponding glutamate-bound structure as described in Experimental Procedures.

the flexibility of the orientation of the lobe structure with respect to the frame of NH vectors described above. Thus, due to the limitations of the experimental data, the structure of glutamate-bound S1S2 could not be determined with a precision greater than that of the crystal structure. However, as described below, using the optimized structures of glutamate-bound protein as a starting point, the differences in lobe orientation between glutamate and a second ligand can be determined with high precision. This is illustrated first for kainate, followed by the application to several willardiine partial agonists and an antagonist.

(ii) Kainate. Kainate is a weak partial agonist of AMPA receptors. The structure of the complex with GluR2 S1S2 suggests a degree of lobe opening[2] relative to glutamate of 10.7 ± 1.1° [calculated with DynDom (*2*)]. The structure seems to be held in this position by what has been termed a foot-in-the-door mechanism (*35*). That is, the isoprenyl group of kainate clashes with Y450 and L650, keeping the lobes from approaching closer. The L650T mutation decreases lobe opening and increases kainate efficacy (*35*). NMR studies using both measurements of tryptophan dynamics [^{19}F NMR spectroscopy (*8*)] and nitrogen relaxation (M. K. Fenwick and R. E. Oswald, unpublished results) suggest that the kainate-bound GluR2 S1S2 structure shows little or no dynamics on the micro- to millisecond time scale and, in fact, is likely to be relatively rigid. Thus, to validate the method, NH RDCs were measured from kainate-bound S1S2 aligned in C12E5/hexanol.

NH RDCs for kainate-bound GluR2 S1S2 were used simply to reorient the lobes of the seven optimized glutamate structures described above. No further optimization was performed; that is, the lobes were reoriented as rigid bodies. Comparing the three glutamate-bound crystal structures (1ftj) with the kainate-bound crystal structure (1fw0), we find the lobe opening (defined relative to glutamate-bound S1S2) is 10.7 ± 1.1° (10.6 ± 1.1° of closure and 0.82 ± 0.75° of twist; see footnote 2 for a description of the components of rotation). Reorienting the refined structures using the kainate RDCs resulted in an opening angle of 11.4 ± 0.3° (10.9 ± 0.2° of closure and 3.1 ± 0.5° of twist). Thus, given what is presumed to be a rather rigid structure, the RDC procedure yields a structure very similar to that observed by crystallography.

The procedure relies on the assumption that the lobes can be reoriented as a rigid body. This is not strictly true, since some portions of the protein exhibit internal motions (*9*−*11*) and, in one case, distinct rotation of the backbone (*1*). However, considering the crystal structure, the internal structure of the core of each lobe remains relatively constant, and via selection of only residues in the core that do not exhibit internal motions, the lobe orientation can be effectively represented. Several lines of evidence support this assumption. Comparing the glutamate-bound structures and the kainate-bound structures and considering the positions of the amide nitrogens for the residues used to reorient the lobe, we find the rmsds are 0.42 ± 0.04 for lobe 1 and 0.36 ± 0.01 for lobe 2. This is on the order of the difference between the different protomers of the glutamate-bound forms (Supporting Information, Table S3) and suggests that the residues chosen in the comparison are consistent with the rigid body assumption. The second line of evidence comes from comparison of the RDC values with the kainate crystal structure. The first step in the procedure uses a large data set (five alignment media) to optimize the glutamate-bound structure to remove structural noise. Considering each lobe individually, the fit of the RDCs obtained from kainate-bound S1S2 to the glutamate-optimized structure can be compared with that to the kainate crystal structures. The fit to the glutamate-optimized structure is significantly better than to the kainate crystal structures (Supporting Information, Tables S1 and S2). Thus, the removal of the structural noise from the glutamate-bound structure also provides a model for the internal structure of each lobe of the kainate-bound structure that is more consistent with the independently measured kainate RDCs than are the kainate crystal struc-

[2] Lobe opening is defined here relative to the C protomer of the glutamate-bound structure [1ftj (*1*)]. In some cases, the term "lobe closure" is used to denote the change from the apo state. Because of the variability of the apo state, lobe opening is used here for quantitative measures, which are obtained using the DomainSelect feature of the DynDom website (http://www.sys.uea.ac.uk/dyndom/) (*2*). DomainSelect calculates the total angle of rotation between two given structures and characterizes the axis of rotation ("screw axis") by the angle relative to the line connecting centers of mass of two specified domains. The total angle of rotation can be decomposed into the closure and twist components. Closure is defined as the rotation that brings centers of mass of the two domains closer, and twist as any rotation perpendicular to closure. A more detailed description of the axes can be obtained at http://www.sys.uea.ac.uk/dyndom/. Note that since a specific protomer of the glutamate-bound structure was used as a reference rather than the apo state, the value of the lobe opening can vary somewhat from that reported by Armstrong and Gouaux (*1*).

tures. The validation of the rigid body assumption for other ligands described below is given in the Supporting Information (Tables S1−S3). Deviations from the rigid body assumption for the residues used in the analysis would significantly affect the results only if the deviations were a result of the concerted movement of a significant portion of the structure which is unlikely [particularly for the willardiine partial agonists described below which show only minor chemical shift changes in the residues that are used (*9*)].

Assuming a rigid body rotation for the residues for which RDC values were used, the degree of lobe opening for the kainate-bound relative to the glutamate-bound structure can be determined with precision for the following reasons. When two arbitrary structures representing S1S2 in different conformations are compared in DynDom (*2*), the program attempts to achieve the best fit of the structure within the corresponding lobes. Consequently, the differences in the intralobe structure directly affect the result of comparison of the relative orientation of the lobes. On the other hand, when two structures related by a rigid body rotation of the lobes are compared, there are no intralobe differences and the comparison most clearly shows the global reorientation. At the same time, a rigid body rotation keeps the NH bond vectors "frozen" with respect to the rest of the structure. That is, the set of vectors representing a lobe will be rotated by the same amount as the lobe as a whole. This fact makes it possible to use DynDom to effectively determine by how much subsets of vectors representing the lobes were rotated between the two structures. Thus, the much larger errors arising from the relationship between NH bond vectors and the rest of the structure (estimated to be approximately ±2°) are not propagated to the difference between the lobe orientations of two structures bound to different ligands, in this case glutamate and kainate.

(iii) Willardiines. Substituted willardiines are a series of natural product analogues (willardiine is the parent compound) that vary from strong partial agonists to full antagonists of AMPA receptors (*20, 21, 40*). For at least the halogen-substituted series, both the binding affinity and the efficacy vary consistently with electronegativity and size of substitutent, respectively. Some evidence suggests that the lobe opening determined from specific group of structures varies linearly with efficacy (*5*). However, the degree of lobe opening varies with crystal conditions, so that it is of interest to determine if such a correlation can exist in solution free of crystal constraints. A series of seven willardiine derivatives were complexed with GluR2 S1S2, aligned in C12E5/hexanol, and NH RDCs measured. As described for kainate, the glutamate-optimized structures were reoriented with the RDC data from the willardiines bound to S1S2 resulting in structures that typically fit the RDC data better than the corresponding crystal structures (Table 2). Among the partial agonists, the variation in lobe opening between willardiine derivatives is small and not significant (ANOVA; $p > 0.05$). The exceptions were BrW and IW for which there are large variabilities in the available crystal structures (Figures 2 and 3). The only antagonist (UBP277) is somewhat less open than the crystal structure determined in zinc solution.

Peptide Flip Region. In addition to large-scale lobe reorientation, one region of the protein has been found by crystallography to exist in at least two different conformations (the peptide flip region). For example, the glutamate-bound structure

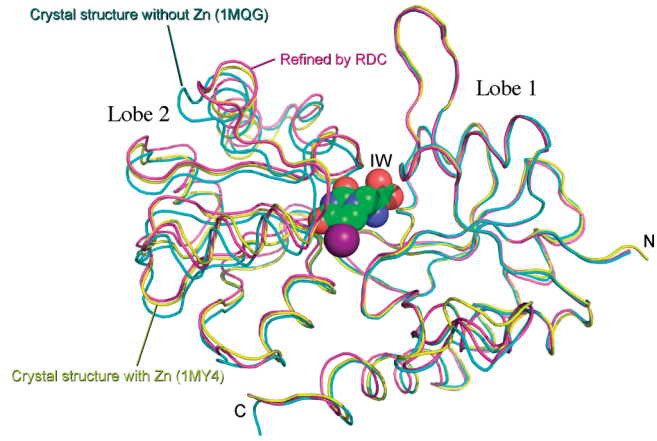

FIGURE 2: Comparison of the IW-bound structures of GluR2 S1S2 aligned along lobe 1, illustrating the differences in lobe orientation. The crystal structure in the presence of Zn [1my4 (*49*)] is colored yellow, the crystal structure in the absence of Zn [1mqg (*5*)] cyan, and the RDC-refined structure magenta.

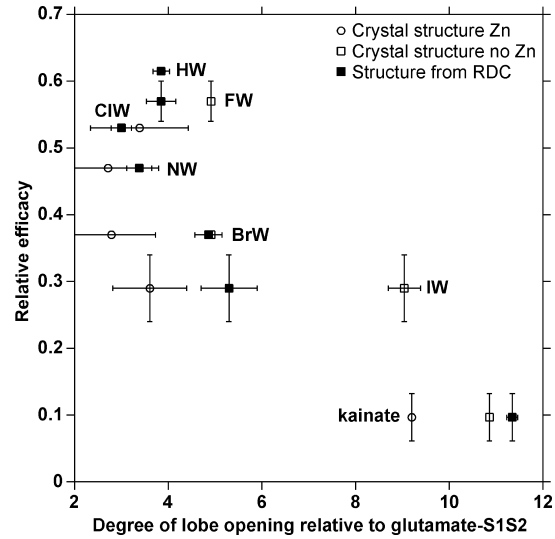

FIGURE 3: Efficacy of willardiine derivatives and kainate as a function of the degree of lobe opening relative to the glutamate-bound structure. The efficacies are taken from refs *5* and *12* and are relative to the full agonist, glutamate. When a given agonist was tested in both studies, the average value was used and the standard error of the mean is shown as the error bar. Lobe opening relative to the corresponding glutamate-bound structure (see Experimental Procedures) is shown as black squares. Crystal structures in the absence of zinc (*1, 5*) are shown as white squares, and those in the presence of zinc (*49*; A. H. Ahmed et al., unpublished observations) are shown as white circles.

(1ftj) exhibits two orientations of the trans peptide bond between D651 and S652 (Figure 4A,B). One protomer is in the "flipped" conformation; one is in the "unflipped" conformation, and a third is poorly defined possibly due to the presence of more than one conformation (*1*). Although the known structures can be classified as flipped, unflipped, or intermediate, the time scale of the interconversion and the relative populations cannot be determined from the crystallographic structures. Because this is a dynamic part of the protein, it was left out of the analysis used in the lobe opening measurements. However, the RDCs from this region can be used to estimate the relative populations and put limits on the time scale of the interconversion.

The time scale of the measurement is set by the frequency of the RDC (on the order of tens of hertz). If the interconversion is fast relative to this time scale, then one peak that

Table 3: Estimates of Populations of the Flipped Conformation (p) in Solution (see the text for a definition of p)[a]

	residue S652				residue G653			
ligand	RDC_{flip}	RDC_{unflip}	$RDC_{measured}$	p	RDC_{flip}	RDC_{unflip}	$RDC_{measured}$	p
glutamate	0.71	−0.11	−	−	1.84	0.22	1.67	0.89
HW	0.78	−0.21	0.33	0.54	1.87	0.22	1.06	0.51
FW	0.78	−0.21	0.23	0.44	1.87	0.22	1.06	0.51
ClW	0.78	−0.20	0.25	0.46	1.86	0.22	1.02	0.49
NW	0.79	−0.23	0.067	0.29	1.87	0.22	0.86	0.39
BrW	0.73	−0.13	0.25	0.45	1.89	0.21	1.08	0.52
IW	0.82	−0.10	0.16	0.28	1.89	0.29	≈0.92	≈0.40
kainate	0.88	−0.30	−0.51	−0.30	1.97	0.23	−0.14	−0.23
		−0.39		**−0.12**		**−0.40**		**0.13**
UBP277	1.05	−0.23	0.12	0.28	2.00	0.36	0.32	−0.02
		−0.43		**0.38**		**−0.42**		**0.31**

[a] The RDCs are normalized by dividing the measured RDC values by the magnitude of the corresponding alignment tensor. For kainate and UBP277, the unflipped structure was also calculated by superimposing the crystal structures for residues L650−S654 of the kainate−S1S2 and UBP277−S1S2 structures on the calculated structures. The RDC values were then predicted and are shown in bold with the corresponding recalculation of p.

is the weighted average of the conformations present is seen. Alternatively, if the time scale of interconversion is slow relative to the RDC, then one set of peaks will be observed for each conformation (e.g., two sets would be observed for a two-site exchange). In all cases, one set of peaks is observed, indicating that either only one conformation is present or the exchange occurs on the time scale of milliseconds or faster.

The optimized glutamate-bound structures included one for which this region is in the flipped conformation and another in the unflipped conformation. As described above, RDCs for each of the partial agonists and the antagonist were used to reorient these structures, so that for each, a flipped and unflipped structure was determined. The NH RDCs from residue G648 to E657 were then predicted for both of the conformations for each compound. The highest level of discrimination for the flipped versus unflipped conformations was for residues S652 and G653. Assuming that flipped and unflipped conformations are the only two long-lived conformations, the population of each can be determined from

$$RDC_{measured} = p \times RDC_{flipped} + (1 - p) \times RDC_{unflipped}$$

The population fraction of flipped conformation p then is given by

$$p = \frac{RDC_{measured} - RDC_{unflipped}}{RDC_{flipped} - RDC_{unflipped}}$$

Table 3 shows the relative populations of each state for peaks that can be measured accurately (those that are significantly exchange broadened or overlapped are excluded). Thus, populations of flipped conformation for different ligands are 89 ± 5% for glutamate, 52 ± 4% for HW, 48 ± 5% for FW, 46 ± 5% for ClW, 48 ± 6% for BrW, 34 ± 4% for NW, and 28 ± 8% for IW (the error estimates are based on the propagation of uncertainties assuming an experimental error of RDC measurement of 1 Hz). The glutamate-bound form significantly favors the flipped form. In fact, a recent high-resolution structure of the glutamate-bound GluR2 S1S2 domain shows three protomers in the flipped form (*39*). The willardiine partial agonists, however, exhibit a stronger tendency to form the unflipped form. In the case of FW, the only crystal structure shows it in the unflipped form, but these data and also data from unpublished HD exchange experiments (M. K. Fenwick and R. E. Oswald, unpublished observations) suggest that the flipped form is also present. For S652 and G653, the kainate- and UBP277-bound forms have RDC values that would fall out of the predicted range. Three crystal structures are available for kainate-bound GluR2 S1S2 (1ftk, 1fw0, and an unpublished structure; A. H. Ahmed and R. E. Oswald, unpublished observations). All show a conformation of the flip region that is slightly different although rather similar to the unflipped form observed with glutamate. The flip region conformation observed in the kainate-bound crystal structures is consistent with RDC measurements, suggesting that the protein is predominantly in the unflipped form when bound to kainate. Likewise, the flip region of the UBP277-bound structures differs from the glutamate-bound structures (Figure 4C). If the flip region conformation observed in the UBP277-bound crystal structure is treated as a more realistic unflipped conformation, the RDCs are consistent with a 60−70% population of the unflipped form. Thus, the RDC measurements can provide a limit on the time scale of the transitions between conformations in this segment of the protein and suggest a dynamic equilibrium that differs among full agonist-, partial agonist-, and antagonist-bound forms.

DISCUSSION

RDCs were used to determine the relative lobe opening of GluR2 S1S2 bound to various agonists and an antagonist relative to the glutamate−S1S2 structure and to estimate the conformational equilibrium of a local conformational transition near the binding site. These studies are a useful complement to the available crystal structures and can help resolve some of the ambiguities arising from differences in structure observed under different crystallization conditions. As we will discuss below, the results suggest that partial agonists of AMPA receptors can function in a manner similar to that of NMDA receptors.

Lobe Orientation. Measurements of the orientation of the two lobes in the S1S2 domain have contributed to the understanding of structure−function relationships in glutamate receptors. For the AMPA receptors, the suggestion has been made that partial agonists can produce a defined degree of lobe orientation that correlates with their efficacy in functional measurements of the intact protein (*5*), although the stability of the closed cleft form has also been proposed as an important factor (*41, 42*). For NMDA receptors, both partial and full agonists have been shown to exhibit full lobe

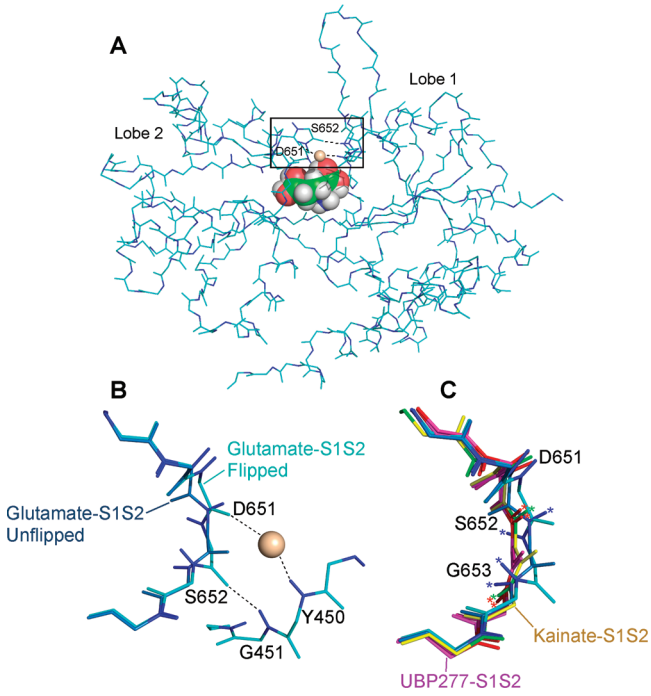

FIGURE 4: Structures of the peptide flip region of GluR2 S1S2. (A) The structure of glutamate-bound GluR2 S1S2 [1ftj (*1*)] is shown with the amide nitrogen and proton highlighted in blue. The box shows the position of the peptide flip region. (B) Flipped and unflipped versions of the glutamate-bound structure. The amide nitrogen and proton are highlighted in blue. The hydrogen bonds formed across the lobe interface are indicated. In the case of D651 and Y450, the hydrogen bond is mediated by a water molecule, which is shown as a tan sphere. (C) Superimposion of the glutamate-bound structures shown in panel B with the kainate-bound structure [1fw0 (*1*)] and two UBP277-bound structures (A. H. Ahmed et al., unpublished observations). The orientation of the amide bond for S652 and G653 differs for the kainate- and UBP277-bound structures from either the flipped or the unflipped conformation of the glutamate-bound structure (denoted with asterisks).

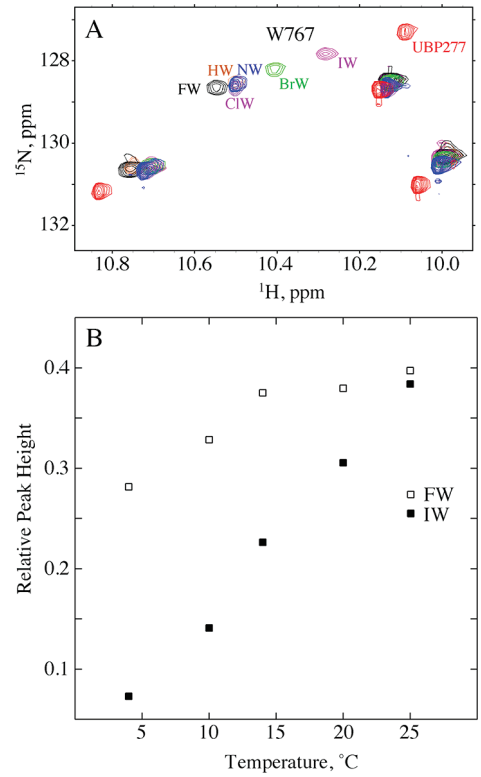

FIGURE 5: (A) Tryptophan side chain region of the ^{1}H−^{15}N TROSY spectrum of GluR2 S1S2 bound to each of the compounds in the willardiine series. (B) Relative intensity of the W767 peak as a function of temperature for FW and IW. The peak height of W767 was normalized to the height of the tryptophan peak at 10.15 ppm.

closure, and either subtle differences in the complex or the stability of the fully closed state determines the efficacy (*43, 44*). An important question is whether the activation of AMPA receptors is fundamentally different from that of NMDA receptors. Crystal structures were used to develop the correlation between lobe orientation and efficacy for AMPA receptors, but considering all available structures for the willardiine partial agonists (Figure 3), the correlation is less obvious.

The method we have developed produces a highly accurate measure of relative lobe orientation, that is, the difference between conformations observed with two different ligands (e.g., partial agonists relative to the full agonist, glutamate). The absolute conformation determined for glutamate is similar to what is observed by crystallography, while having a range of lobe openings no different from that observed in the different crystal forms. For the partial agonists and the antagonist, lobe opening relative to glutamate is either identical to that measured in the available crystal structures or within the range of openings that have been measured in different forms. BrW, kainate, and IW have been crystallized both in the presence and in the absence of zinc. S1S2 bound to ClW, HW, NW, and UBP277 has been crystallized only in the presence of zinc, and S1S2 bound to FW has been crystallized only in the absence of zinc. The UBP277-bound structure is similar both in solution and in the crystal structure. This seems to be due largely to the steric effects of the carboxyethyl group that prevents further lobe closure. Except for the IW-bound structure in the absence of zinc, the remainder of the willardiine structures both in solution and in the crystal has relatively small openings (2.5−5.5° relative to the C protomer of the glutamate-bound 1ftj), with no clear dependency of efficacy on lobe orientation. The measurements in solution are consistently more open than the zinc-containing crystal structures and clearly more closed than the zinc-free IW-bound structure. The differences between the solution and crystal structures could be due simply to the restraints of crystal packing that are not present in solution. Alternatively, the multiple orientations observed between crystal forms and between the crystal and solution forms could potentially reflect an ensemble of lobe orientations that exist in solution.

Howe and collaborators (*42, 45*) have suggested that the stability of the interface between lobes determines efficacy, and if this is true, one consequence might be a larger distribution of lobe openings for partial agonists. This cannot be directly observed in the crystal structures, but a hydrogen bond made by the side chain of W767 shows clear differences between willardiine partial agonists of different efficacies. As shown in Figure 5A, the chemical shift of the W767 side chain NH group varies with substituent on the willardiine ring. For complexes with higher-efficacy willardiine derivatives (HW, FW, ClW, and NW), the chemical shifts are very similar. However, the chemical shift moves progressively upfield for BrW, IW, and UBP277. The W767 (lobe 1) side chain NH group forms a hydrogen bond with the backbone carbonyl of T707 (lobe 2). Changes in chemical

shift can arise from a number of factors, but for amide protons involved in hydrogen bonds, the lengthening of the hydrogen bond has been correlated to an upfield shift (*46*). T707 is on the rotation axis, so that small displacements are propagated to the remainder of lobe 2 as larger rotations. Because of this, the hydrogen bond even in the relatively open UBP277-bound structure can be maintained. The simple change in chemical shift is consistent with a more open structure for BrW, IW, and UBP277; however, the temperature dependence of the peak can provide some information about dynamics. The intensity of the peak is inversely related to line width that normally broadens with a decrease in temperature. As shown in Figure 5B, the peak intensity decreases much more dramatically for IW than for FW. This relative decrease in intensity can be related to an increase in the level of chemical exchange on the micro- to millisecond time scale (*9*). One interpretation would be that the lower-efficacy partial agonists in the willardiine series would have less stable closed states and a wider range of lobe opening angles than the higher-efficacy partial agonists.

The analysis of various mutations has also brought into question a direct relationship between a fixed lobe orientation and efficacy. L650T partially removes the steric constraints on lobe closing in the presence of kainate and is activated with higher efficacy with this partial agonist. More interestingly, AMPA becomes a partial agonist, and the ensemble of crystal structures show that a range of lobe opening from fully closed to ≈10° open can be observed (*35*). Although this is a mutated receptor, it does illustrate the point that in going from a full to a partial agonist, additional degrees of lobe opening become populated as part of an ensemble. The T686A mutation does not change the degree of lobe opening measured by crystallography but does decrease the level of interlobe hydrogen bonding and decreases the efficacy for glutamate and quisqualate (*45*).

The important challenge is to relate these data to the functional properties of AMPA receptors. AMPA receptors are tetramers, with four potential binding sites for an agonist (one on each of the four S1S2 domains). Single-channel recording suggests that three conductance levels can be observed, with the highest conductance more likely to be populated at high agonist concentrations (*47*). A plausible model is that agonists bound to two subunits are required to produce a measurable channel opening and that the binding of the third and fourth produces successively larger conductance openings, possibly by increasing the size of the pore further or possibly by changing its charge configuration (*48*). Partial agonists differ from full agonists by preferentially populating the lower-conductance states even at saturating concentrations. Thus, partial agonism arises from a less efficient coupling between binding and channel opening. Jin et al. (*5*) suggested introduction of an efficacy factor that was related to the orientation of the lobes. This was an elegant solution but left vague the physical mechanism by which the degree of lobe closure gives rise to the efficacy factor. The results presented here do not necessarily support a simple relationship between a stable lobe orientation and efficacy. Indeed, for most willardiines, the average lobe orientation in solution appears to be nearly the same, while their efficacies vary considerably (Figure 3). For BrW and IW, a variety of data suggests that a range of lobe orientations may exist. This conclusion is consistent with the range of lobe opening angles measured by crystallography and NMR, the chemical exchange observed in a hydrogen bond across the lobe interface, and the equilibrium between flipped and unflipped conformations that add and subtract hydrogen bonds from the interface between the two lobes. Such an ensemble may be a consequence of the reduced stability of the lobe interface in partial agonists. This could in turn decrease efficacy by decreasing the proportion of time spent in a conformation permissible for channel opening.

Peptide Flip Region. The peptide flip region is near the agonist binding site and can differentially stabilize the closed lobe state by forming two additional hydrogen bonds in the flipped but not the unflipped state (Figure 4B). Clearly, the protein is capable of assuming at least these two conformations, but the relative populations of the two states or the kinetics of the transition are not known. Indirect measurements with [^{19}F]tryptophan suggested that the transition rates for the IW- and BrW-bound forms may be less than 10000 Hz. In this case, RDCs can establish only a lower boundary for the transition rate. Since only a single peak is observed for each of the residues in the flip region, the transition would be significantly faster than 30 Hz, at least consistent with other measurements.

The population distribution can also be estimated, assuming a two-state model. Although an unflipped form is seen in one protomer of the crystal structure, the RDC data suggest that the flipped form predominates for the glutamate−S1S2 structure. The FW− and ClW−S1S2 complexes seem to have roughly equal populations of the two forms. Note that only one crystal structure is known for FW and it is in the unflipped form. NW and IW structures show approximately one-third flipped and two-thirds unflipped. The flipped and unflipped crystal structure for glutamate is locally almost superimposable on the willardiine partial agonist structures. On the other hand, the flip regions for the kainate- and UBP277-bound forms (both unflipped in all structures) are somewhat different from that for glutamate in the unflipped form (Figure 4). The actual structure of the flip region for the kainate-bound structure is consistent with RDC data and thus indicates a largely unflipped form of the protein. In the case of UBP277, the RDCs are consistent with a mixture of flipped and unflipped forms, although it is not clear if the hydrogen bonds characteristic of the flipped form could be formed with UBP277 in the binding site. To the extent that the flip region stabilizes the lobe interface, one might expect the flipped form to predominate in full agonists, be intermediate in partial agonists, and be largely nonexistent in weak partial agonists and antagonists. With the exception of UBP277, this trend seems to hold using RDC measurements.

CONCLUSIONS

RDC measurements can be used not only to provide orientational constraints on protein structures in terms of large-scale orientation of domains but also to predict the average orientation of specific bond vectors. Lobe orientation in the binding domain of AMPA receptors has been the basis for building structure−function models of this crucial neurotransmitter receptor. Because of lobe orientation measurements in some crystal structures, the proposal has been made that AMPA receptors are fundamentally different from NMDA receptors (*44*). For NMDA receptors, partial agonists

can induce a full lobe closure and the stability of this state may be related to efficacy. For AMPA receptors, the halogenated willardiine series has been used to make the case that a stable lobe orientation is correlated with efficacy. However, the correlation is less obvious if crystals formed in zinc are considered. The results presented here suggest that the average solution conformations for the willardiine partial agonists are not strongly correlated with efficacy and, where data are available, the conformation lies between the crystal structures determined in the presence and absence of zinc. In isolation, these results might reflect either a stable conformation or the average of a dynamic equilibrium. When the crystal structures and stability of hydrogen bonds across the lobe interface (both W767−T707 and the flip region H bonds) are considered, an attractive hypothesis is that the results reflect a dynamic equilibrium for which the crystal structures reveal different members of the ensemble. On the basis of this, partial agonism may arise from the decreased proportion of time spent in a conformation permissive to channel opening. Thus, NMR-derived RDC constraints can be used to complement structures obtained by X-ray crystallography and may help provide links to the function of AMPA receptors.

ACKNOWLEDGMENT

We thank Prof. Eric Gouaux (Vollum Institute) for the GluR2 S1S2J construct and Prof. Adrienne Loh (University of Wisconsin, LaCrosse, WI), Prof. Linda Nicholson (Cornell University), Prof. Linda Nowak (Cornell University), and Dr. Chris Ptak (Cornell University) for useful discussions and important advice.

SUPPORTING INFORMATION AVAILABLE

Comparison of RDC values to each lobe individually (Tables S1 and S2), pairwise comparison (rmsd, in angstroms) of the individual lobes of the glutamate-bound S1S2 structures with the corresponding lobes from structures of S1S2 bound to various ligands (Table S3), and data from $^{1}H-^{15}N$ TROSY experiments illustrating the determination of RDC values (Figure S1). This material is available free of charge via the Internet at http://pubs.acs.org.

REFERENCES

1. Armstrong, N., and Gouaux, E. (2000) Mechanisms for activation and antagonism of an AMPA-sensitive glutamate receptor: Crystal structures of the GluR2 ligand binding core. *Neuron 28*, 165–181.
2. Hayward, S., and Lee, R. A. (2002) Improvements in the analysis of domain motions in proteins from conformational change: DynDom version 1.50. *J. Mol. Graphics Modell. 21*, 181–183.
3. Dingledine, R., Borges, K., Bowie, D., and Traynelis, S. (1999) The glutamate receptor ion channels. *Pharmacol. Rev. 51*, 7–61.
4. Asztely, F., and Gustafsson, B. (1996) Ionotropic glutamate receptors. Their possible role in the expression of hippocampal synaptic plasticity. *Mol. Neurobiol. 12*, 1–11.
5. Jin, R., Banke, T. G., Mayer, M. L., Traynelis, S. F., and Gouaux, E. (2003) Structural basis for partial agonist action at ionotropic glutamate receptors. *Nat. Neurosci. 6*, 803–810.
6. Sun, Y., Olson, R., Horning, M., Armstrong, N., Mayer, M., and Gouaux, E. (2002) Mechanism of glutamate receptor desensitization. *Nature 417*, 245–253.
7. Armstrong, N., Sun, Y., Chen, G. Q., and Gouaux, E. (1998) Structure of a glutamate-receptor ligand-binding core in complex with kainate. *Nature 395*, 913–917.
8. Ahmed, A. H., Loh, A. P., Jane, D. E., and Oswald, R. E. (2007) Dynamics of the S1S2 glutamate binding domain of GluR2 measured using ^{19}F NMR spectroscopy. *J. Biol. Chem. 282*, 12773–12784.
9. Fenwick, M. K., and Oswald, R. E. (2008) NMR spectroscopy of the ligand-binding core of ionotropic glutamate receptor 2 bound to 5-substituted willardiine partial agonists. *J. Mol. Biol. 378*, 673–685.
10. McFeeters, R. L., and Oswald, R. E. (2002) Structural mobility of the extracellular ligand-binding core of an ionotropic glutamate receptor. Analysis of NMR relaxation dynamics. *Biochemistry 41*, 10472–10481.
11. Valentine, E. R., and Palmer, A. G. (2005) Microsecond-to-millisecond conformational dynamics demarcate the GluR2 glutamate receptor bound to agonists glutamate, quisqualate, and AMPA. *Biochemistry 44*, 3410–3417.
12. Mankiewicz, K. A., Rambhadran, A., Wathen, L., and Jayaraman, V. (2008) Chemical interplay in the mechanism of partial agonist activation in α-amino-3-hydroxy-5-methyl-4-isoxazolepropionic acid receptors. *Biochemistry 47*, 398–404.
13. Mankiewicz, K. A., Rambhadran, A., Du, M., Ramanoudjame, G., and Jayaraman, V. (2007) Role of the chemical interactions of the agonist in controlling α-amino-3-hydroxy-5-methyl-4-isoxazolepropionic acid receptor activation. *Biochemistry 46*, 1343–1349.
14. Jayaraman, V. (2004) Spectroscopic and kinetic methods for ligand-protein interactions of glutamate receptor. *Methods Enzymol. 380*, 170–187.
15. Arinaminpathy, Y., Sansom, M. S., and Biggin, P. C. (2002) Molecular Dynamics Simulations of the Ligand-Binding Domain of the Ionotropic Glutamate Receptor GluR2. *Biophys. J. 82*, 676–683.
16. Lau, A. Y., and Roux, B. (2007) The free energy landscapes governing conformational changes in a glutamate receptor ligand-binding domain. *Structure 15*, 1203–1214.
17. Mamonova, T., Hespenheide, B., Straub, R., Thorpe, M. F., and Kurnikova, M. (2005) Protein flexibility using constraints from molecular dynamics simulations. *Phys. Biol. 2*, S137–S147.
18. Tjandra, N., Garrett, D. S., Gronenborn, A. M., Bax, A., and Clore, G. M. (1997) Defining long range order in NMR structure determination from the dependence of heteronuclear relaxation times on rotational diffusion anisotropy. *Nat. Struct. Biol. 4*, 443–449.
19. Tjandra, N., Omichinski, J. G., Gronenborn, A. M., Clore, G. M., and Bax, A. (1997) Use of dipolar $^{1}H-^{15}N$ and $^{1}H-^{13}C$ couplings in the structure determination of magnetically oriented macromolecules in solution. *Nat. Struct. Biol. 4*, 732–738.
20. Dolman, N. P., Troop, H. M., More, J. C., Alt, A., Knauss, J. L., Nistico, R., Jack, S., Morley, R. M., Bortolotto, Z. A., Roberts, P. J., Bleakman, D., Collingridge, G. L., and Jane, D. E. (2005) Synthesis and pharmacology of willardiine derivatives acting as antagonists of kainate receptors. *J. Med. Chem. 48*, 7867–7881.
21. Jane, D. E., Hoo, K., Kamboj, R., Deverill, M., Bleakman, D., and Mandelzys, A. (1997) Synthesis of willardiine and 6-azawillardiine analogs: Pharmacological characterization on cloned homomeric human AMPA and kainate receptor subtypes. *J. Med. Chem. 40*, 3645–3650.
22. Hollmann, M., and Heinemann, S. (1994) Cloned glutamate receptors. *Annu. Rev. Neurosci. 17*, 31–108.
23. Chen, G. Q., and Gouaux, E. (1997) Overexpression of a glutamate receptor (GluR2) ligand binding domain in *Escherichia coli*: Application of a novel protein folding screen. *Proc. Natl. Acad. Sci. U.S.A. 94*, 13431–13436.
24. Maniatis, T., Fritsch, E. F., and Sambrook, J. (1982) *Molecular Cloning*, Cold Spring Harbor Laboratory Press, New York.
25. Delaglio, F., Grzesiek, S., Vuister, G. W., Zhu, G., Pfeifer, J., and Bax, A. (1995) NMRPipe: A multidimensional spectral processing system based on UNIX pipes. *J. Biomol. NMR 6*, 277–293.
26. Goddard, T. D., and Kneller, D. G. (2003) *SPARKY 3*, University of California, San Francisco.
27. Ruckert, M., and Otting, G. (2000) Alignment of biological macromolecules in novel nonionic liquid crystalline media for NMR experiments. *J. Am. Chem. Soc. 122*, 7793–7797.
28. Wang, H., Eberstadt, M., Olejniczak, E. T., Meadows, R. P., and Fesik, S. W. (1998) A liquid crystalline medium for measuring residual dipolar couplings over a wide range of temperatures. *J. Biomol. NMR 12*, 443–446.
29. Ishii, Y., Markus, M. A., and Tycko, R. (2001) Controlling residual dipolar couplings in high-resolution NMR of proteins by strain induced alignment in a gel. *J. Biomol. NMR 21*, 141–151.

30. Barrientos, L. G., Dolan, C., and Gronenborn, A. M. (2000) Characterization of surfactant liquid crystal phases suitable for molecular alignment and measurement of dipolar couplings. *J. Biomol. NMR 16*, 329–337.
31. Ulmer, T. S., Ramirez, B. E., Delaglio, F., and Bax, A. (2003) Evaluation of backbone proton positions and dynamics in a small protein by liquid crystal NMR spectroscopy. *J. Am. Chem. Soc. 125*, 9179–9191.
32. Schwieters, C. D., Kuszewski, J. J., Tjandra, N., and Clore, G. M. (2003) The Xplor-NIH NMR molecular structure determination package. *J. Magn. Reson. 160*, 65–73.
33. Tolman, J. R. (2002) A novel approach to the retrieval of structural and dynamic information from residual dipolar couplings using several oriented media in biomolecular NMR spectroscopy. *J. Am. Chem. Soc. 124*, 12020–12030.
34. Fenwick, M. K., and Oswald, R. E. (2008) Backbone chemical shift assignment of a glutamate receptor ligand binding domain in complexes with five partial agonists. *Biomol. NMR Assignments 1*, 241–243.
35. Armstrong, N., Mayer, M., and Gouaux, E. (2003) Tuning activation of the AMPA-sensitive GluR2 ion channel by genetic adjustment of agonist-induced conformational changes. *Proc. Natl. Acad. Sci. U.S.A. 100*, 5736–5741.
36. Wang, Y. X., Marquardt, J. L., Wingfield, P. T., Stahl, S. J., Lee-Huang, S., Torchia, D. A., and Bax, A. (1998) Simultaneous measurement of ^{1}H-^{15}N, ^{1}H-$^{13}C'$, and ^{15}N-$^{13}C'$ dipolar couplings in a perdeuterated 30 kDa protein dissolved in a dilute liquid crystalline phase. *J. Am. Chem. Soc. 120*, 7385–7386.
37. Skrynnikov, N. R., Goto, N. K., Yang, D., Choy, W. Y., Tolman, J. R., Mueller, G. A., and Kay, L. E. (2000) Orienting domains in proteins using dipolar couplings measured by liquid-state NMR: Differences in solution and crystal forms of maltodextrin binding protein loaded with β-cyclodextrin. *J. Mol. Biol. 295*, 1265–1273.
38. Tolman, J. R., Al-Hashimi, H. M., Kay, L. E., and Prestegard, J. H. (2001) Structural and dynamic analysis of residual dipolar coupling data for proteins. *J. Am. Chem. Soc. 123*, 1416–1424.
39. Ahmed, A. H., Wang, Q., Sondermann, H., and Oswald, R. E. (2008)Structure of the S1S2 glutamate binding domain of GluR3, submitted for publication.
40. Patneau, D. K., Mayer, M. L., Jane, D. E., and Watkins, J. C. (1992) Activation and desensitization of AMPA/kainate receptors by novel derivatives of willardiine. *J. Neurosci. 12*, 595–606.
41. Mayer, M. L. (2006) Glutamate receptors at atomic resolution. *Nature 440*, 456–462.
42. Robert, A., Armstrong, N., Gouaux, J. E., and Howe, J. R. (2005) AMPA receptor binding cleft mutations that alter affinity, efficacy, and recovery from desensitization. *J. Neurosci. 25*, 3752–3762.
43. Furukawa, H., and Gouaux, E. (2003) Mechanisms of activation, inhibition and specificity: Crystal structures of the NMDA receptor NR1 ligand-binding core. *EMBO J. 22*, 2873–2885.
44. Inanobe, A., Furukawa, H., and Gouaux, E. (2005) Mechanism of partial agonist action at the NR1 subunit of NMDA receptors. *Neuron 47*, 71–84.
45. Zhang, W., Cho, Y., Lolis, E., and Howe, J. R. (2008) Structural and single-channel results indicate that the rates of ligand binding domain closing and opening directly impact AMPA receptor gating. *J. Neurosci. 28*, 932–943.
46. Wagner, G., Pardi, A., and Wuthrich, K. (1983) Hydrogen-Bond Length and H-1-NMR Chemical Shifts in Proteins. *J. Am. Chem. Soc. 105*, 5948–5949.
47. Rosenmund, C., Stern-Bach, Y., and Stevens, C. F. (1998) The tetrameric structure of a glutamate receptor channel. *Science 280*, 1596–1599.
48. Oswald, R. E. (2004) Ionotropic glutamate receptor recognition and activation. *Adv. Protein Chem. 68*, 313–349.
49. Jin, R., and Gouaux, E. (2003) Probing the function, conformational plasticity, and dimer-dimer contacts of the GluR2 ligand-binding core: Studies of 5-substituted willardiines and GluR2 S1S2 in the crystal. *Biochemistry 42*, 5201–5213.

BI800843C